

## Efficient Incorporation of a Copper Hydroxypyridone Base Pair in DNA

Kentaro Tanaka,<sup>†</sup> Atsushi Tengeiji,<sup>†</sup> Tatsuhisa Kato,<sup>‡</sup> Namiki Toyama,<sup>‡</sup>  
Motoo Shiro,<sup>§</sup> and Mitsuhiro Shionoya<sup>\*†</sup>

Contribution from the Department of Chemistry, Graduate School of Science,  
The University of Tokyo, Hongo, Bunkyo-ku, Tokyo 113-0033, Japan,  
Institute for Molecular Science, Myodaiji, Okazaki 444-8585, Japan, and  
Rigaku Corporation, 3-9-12 Matsubaracho, Akishima, Tokyo 196-8666, Japan

Received June 5, 2002

**Abstract:** Recently, we reported the first artificial nucleoside for alternative DNA base pairing through metal complexation (*J. Org. Chem.* **1999**, *64*, 5002–5003). In this regard, we report here the synthesis of a hydroxypyridone-bearing nucleoside and the incorporation of a neutral Cu<sup>2+</sup>-mediated base pair of hydroxypyridone nucleobases (H–Cu–H) in a DNA duplex. When the hydroxypyridone bases are incorporated into the middle of a 15 nucleotide duplex, the duplex displays high thermal stabilization in the presence of equimolar Cu<sup>2+</sup> ions in comparison with a duplex containing an A–T pair in place of the H–H pair. Monitoring temperature dependence of UV-absorption changes verified that a Cu<sup>2+</sup>-mediated base pair is stoichiometrically formed inside the duplex and dissociates upon thermal denaturation at elevated temperature. In addition, EPR and CD studies suggested that the radical site of a Cu<sup>2+</sup> center is formed within the right-handed double-strand structure of the oligonucleotide. The present strategy could be developed for controlled and periodic spacing of neutral metallobase pairs along the helix axis of DNA.

### Introduction

Efforts toward the expansion of the genetic alphabet have been made extensively with respect to artificial gene control as well as development of functionalized biopolymers.<sup>1,2</sup> Recently, we<sup>3</sup> and others<sup>4,5</sup> have reported a few examples of alternative

base-pairing modes in which hydrogen-bonded base pairs present in natural DNA are replaced by metal-mediated ones. Along this strategy, we have designed a novel hydroxypyridone nucleobase (H) as a planar bidentate ligand (Chart 1). Since hydroxypyridone is known to form, with concomitant deprotonation, a stable, neutral complex with a divalent transition metal ion such as Cu<sup>2+</sup>,<sup>6</sup> the resulting square-planar complex should replace hydrogen-bonded natural base pairs. We report here the synthesis of hydroxypyridone-bearing nucleoside **1**, efficient incorporation of **1** into oligonucleotides, **2** and **3**, and the influence of a copper-mediated pair of the chelator-type nucleobases on the thermal stability of the DNA duplex.

### Results and Discussion

A synthetic route for a hydroxypyridone-bearing nucleoside **1** is shown in Scheme 1. A key step was a Lewis acid-catalyzed coupling reaction<sup>7</sup> between fully protected deoxyribofuranose **6**<sup>8</sup> and 2-methyl-3-(benzyloxy)-4-pyridone (**7**).<sup>9</sup> The resulting mixture of  $\alpha$ - and  $\beta$ -anomers **8** ( $\alpha$ : $\beta$  = 3:7) was used for the following deprotection without separation. After removal of the benzyl group, the desired  $\beta$ -N-nucleoside **9** was successfully isolated by recrystallization from EtOH, and its anomeric configuration was determined by X-ray crystal analysis (Figure

\* To whom correspondence should be addressed. Phone: +81-3-5841-8061. Fax: +81-3-5841-8061. E-mail: shionoya@chem.s.u-tokyo.ac.jp

<sup>†</sup> The University of Tokyo.

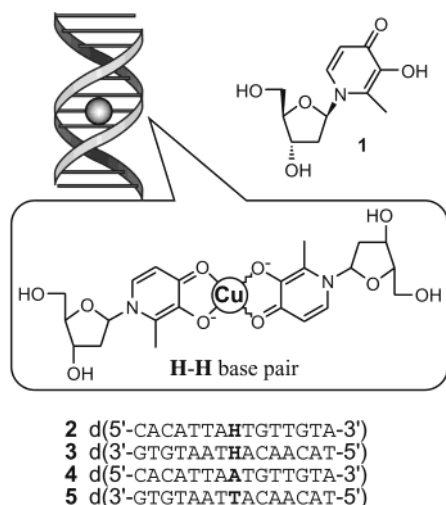
<sup>‡</sup> Institute for Molecular Science.

<sup>§</sup> Rigaku Corporation.

- (1) (a) Switzer, S.; Moroney, S. E.; Benner, S. A. *J. Am. Chem. Soc.* **1989**, *111*, 8322. (b) Piccirilli, J. A.; Krauch, T.; Moroney, S. E.; Benner, S. A. *Nature* **1990**, *343*, 33. (c) Switzer, C. Y.; Moroney, S. E.; Benner, S. A. *Biochemistry* **1993**, *32*, 10489. (d) Horlacher, J.; Hottiger, M.; Podust, V. N.; Hübscher, U.; Benner, S. A. *Proc. Natl. Acad. Sci. U.S.A.* **1995**, *92*, 6329. (e) Lutz, M. J.; Held, H. A.; Hottiger, M.; Hübscher, U.; Benner, S. A. *Nucleic Acids Res.* **1996**, *24*, 1308.
- (2) (a) Kool, E. T. *Biopolymers* **1998**, *48*, 3. (b) Guckian, K. M.; Krugh, T. R.; Kool, E. T. *Nat. Struct. Biol.* **1998**, *11*, 954. (c) Kool, E. T.; Morales, J. C.; Guckian, K. M. *Angew. Chem., Int. Ed.* **2000**, *39*, 990. (d) McMinn, D. L.; Ogawa, A. K.; Wu, Y.; Liu, J.; Schultz, P. G.; Romesberg, F. E. *J. Am. Chem. Soc.* **1999**, *121*, 11585. (e) Ogawa, A. K.; Wu, Y.; McMinn, D. L.; Liu, J.; Schultz, P. G.; Romesberg, F. E. *J. Am. Chem. Soc.* **2000**, *122*, 3274. (f) Wu, Y.; Ogawa, A. K.; Berger, M.; McMinn, D. L.; Schultz, P. G.; Romesberg, F. E. *J. Am. Chem. Soc.* **2000**, *122*, 7621. (g) Brotschi, C.; Häberli, A.; Leumann, C. J. *Angew. Chem., Int. Ed.* **2001**, *40*, 3012.
- (3) (a) Tanaka, K.; Shionoya, M. *J. Org. Chem.* **1999**, *64*, 5002. (b) Cao, H.; Tanaka, K.; Shionoya, M. *Chem. Pharm. Bull.* **2000**, *48*, 1745. (c) Shionoya, M.; Tanaka, K. *Bull. Chem. Soc. Jpn.* **2000**, *73*, 1945. (d) Tanaka, K.; Tasaka, M.; Cao, H.; Shionoya, M. *Eur. J. Pharm. Sci.* **2001**, *13*, 77. (e) Tasaka, M.; Tanaka, K.; Shiro, M.; Shionoya, M. *Supramol. Chem.* **2001**, *13*, 671. (f) Tanaka, K.; Tasaka, M.; Cao, H.; Shionoya, M. *Supramol. Chem.* **2002**, *14*, 255. (g) Tanaka, K.; Yamada, Y.; Shionoya, M. *J. Am. Chem. Soc.* **2002**, *124*, 8802.
- (4) (a) Meggers, E.; Holland, P. L.; Tolman, W. B.; Romesberg, F. E.; Schultz, P. G. *J. Am. Chem. Soc.* **2000**, *122*, 10714. (b) Atwell, S.; Meggers, E.; Spraggon, G.; Schultz, P. G. *J. Am. Chem. Soc.* **2001**, *123*, 12364.
- (5) (a) Weizman, H.; Tor, Y. *Chem. Commun.* **2001**, 453. (b) Weizman, H.; Tor, Y. *J. Am. Chem. Soc.* **2001**, *123*, 3375.

- (6) (a) El-Jammal, A.; Howell, P. L.; Turner, M. A.; Li, N.; Templeton, D. M. *J. Med. Chem.* **1994**, *37*, 461. Here the X-ray structure of a square-planar Cu<sup>2+</sup> complex in the trans form is reported. (b) Ahmed, S. I.; Burgess, J.; Fawcett, J.; Parsons, S. A.; Russell, D. R.; Laurie, S. H. *Polyhedron* **2000**, *19*, 129. (c) Griffith, W. P.; Mostafa, S. I. *Polyhedron* **1992**, *11*, 2997.
- (7) Mao, D. T.; Driscoll, J. S.; Marquez, V. S. *J. Med. Chem.* **1984**, *27*, 160.
- (8) Gold, A.; Sangaiah, R. *Nucleosides Nucleotides* **1990**, *9*, 907.
- (9) Harris, R. L. *N. Aust. J. Chem.* **1976**, *29*, 1329.

Chart 1



1).<sup>10</sup> After removal of the acetyl groups, the 5' and phenolic hydroxy groups of **1** were selectively protected in order by 4,4'-dimethoxytrityl and pivaloyl groups, respectively. Nucleoside **11** thus obtained was finally converted to phosphoramidite **12**. Incorporation into oligodeoxynucleotides and deprotection of the fully protected products were carried out with standard protocols using an automated DNA synthesizer.

We have chosen a  $\text{Cu}^{2+}$  ion that forms a 1:2 square-planar complex with deprotonated hydroxypyridone ligands.<sup>6a</sup> UV-absorption change upon complexation was employed as a quantitative structural probe to verify the presence of bound  $\text{Cu}^{2+}$  ions. Figure 2 shows UV-absorption changes of **1** when the concentration of  $\text{Cu}^{2+}$  ions is increased. With an increase in the  $\text{Cu}^{2+}$  concentration, the absorbance at 282 nm gradually decreased while a new peak at 303 nm appeared with two isosbestic points in the range of  $[\text{Cu}^{2+}]/[\mathbf{1}]$  from 0.0 to 0.5. This simultaneous change indicates the deprotonation of phenolic hydroxy groups of hydroxypyridone ligands upon  $\text{Cu}^{2+}$  complexation. Absorption data at 282 and 303 nm are plotted as a function of the ratio of  $\text{Cu}^{2+}$  to **1** (Figure 2, inset), clearly showing the complex formation between  $\text{Cu}^{2+}$  and hydroxypyridone ligand **1** in a 1:2 ratio. The final product was confirmed by electrospray ionization time-of-flight mass spectrometry (found,  $m/z$  566.10, calcd for  $[\text{M} + \text{Na}]^+$ ,  $m/z$  566.09, where M represents a 1:2 complex,  $\text{Cu}^{2+} \cdot 2(\mathbf{1} - \text{H}^+)$ ).

To examine the influence of  $\text{Cu}^{2+}$  ions on the thermal stability of an H-H base pair in DNA, the pair was introduced in the middle of a 15-nucleotide DNA duplex (**2·3**), d(5'-CACATTAHTGTTGTA-3')·d(3'-GTGTAATHACAACAT-5'), and the melting temperature in the absence or presence of  $\text{Cu}^{2+}$  ions was determined by UV-monitored thermal denaturation ([duplex] = 2  $\mu\text{M}$ ). In the absence of  $\text{Cu}^{2+}$  ions, the duplex **2·3** showed a melting temperature of 37.0 °C (Figure 3a), whereas

a natural-type oligoduplex (**4·5**), d(5'-CACATTAATGTTGTA-3')·d(3'-GTGTAATTACAACAT-5'), in which the H-H base pair is replaced by an A-T base pair, melted at 44.2 °C (Figure 3b). Thus, in the absence of  $\text{Cu}^{2+}$  ions, the H-H base pair behave as a mispair to destabilize the duplex, although the pair could possibly be hydrogen-bonded (Figure 1). In contrast, addition of equimolar  $\text{Cu}^{2+}$  ions (2  $\mu\text{M}$ ) to the duplex **2·3** led to base pairing with higher thermal stability. Thermal denaturation of **2·3** resulted in a biphasic melting curve with a melting point of 50.1 °C (Figure 3c), which is higher than that of **4·5** in the absence of  $\text{Cu}^{2+}$  ions. Thus, the  $\text{Cu}^{2+}$ -assisted base pair in **2·3** stabilized the duplex by about 13 °C,<sup>11</sup> whereas the natural duplex **4·5** was hardly affected by addition of  $\text{Cu}^{2+}$  ions (Figure 3d).

Figure 4 shows the temperature dependence of the UV absorption for the duplex **2·3** in the presence of equimolar  $\text{Cu}^{2+}$  ions ( $[\mathbf{2} \cdot \mathbf{3}] = [\text{Cu}^{2+}] = 2 \mu\text{M}$ ). As is evidenced in Figure 4a, a peak at 314 nm that appeared at low temperature indicates that  $\text{Cu}^{2+}$  ions interact preferentially with the hydroxypyridone moiety and that the resulting  $\text{Cu}^{2+}$ -mediated base pair (H-Cu-H) is stoichiometrically formed inside the duplex.<sup>12</sup> As the temperature was raised from 10 to 85 °C, this peak at 314 nm characteristic for the  $\text{Cu}^{2+}$  complex gradually disappeared, where absorbance at 260 nm simultaneously increased with two isosbestic points as shown in Figure 4a. Absorption changes ( $\Delta A/\Delta A_{\text{max}}$  from 10 to 85 °C) at 260 nm (broken line in Figure 4b) are in fair agreement with those at 314 nm (solid line in Figure 4b). This result suggests that, at elevated temperature after melting, the hydroxypyridone bases no longer bind to  $\text{Cu}^{2+}$  ions.

The circular dichroism (CD) spectrum of the duplex **2·3** without  $\text{Cu}^{2+}$  ion has a characteristic feature of typical right-handed B-DNA (Figure 5).<sup>13</sup> The metalloduplex showed almost the same spectrum except an additional positive Cotton effect was observed at 314 nm (Figure 5, solid line). This result indicates that a  $\text{Cu}^{2+}$ -hydroxypyridone complex incorporated hardly affects the B-DNA helix sense.

Electron paramagnetic resonance (EPR) was used as a quantitative structural probe to verify the presence of bound  $\text{Cu}^{2+}$  ions. The X-band EPR spectrum at 1.5 K of a frozen aqueous solution of the duplex **2·3** with equimolar  $\text{Cu}^{2+}$  ions is compared with that of a 1:2  $\text{Cu}^{2+}$ -complex with mononucleoside **1** (Figure 6). Both spectra are comparable with those of  $\text{Cu}^{2+}$ -porphyrins<sup>14</sup> and are due to a doublet ( $S = 1/2$ ) radical of a  $\text{Cu}^{2+}$  center in the square-planar ligand field. A significant difference was the line sharpening of the spectrum of the  $\text{Cu}^{2+}$  complex with the duplex **2·3**. This line sharpening could reflect the isolation of the radical site from hydrated water into the hydrophobic environment. This fact suggests that the radical site of a  $\text{Cu}^{2+}$  center is formed within the right-handed double-strand structure of oligonucleotide.

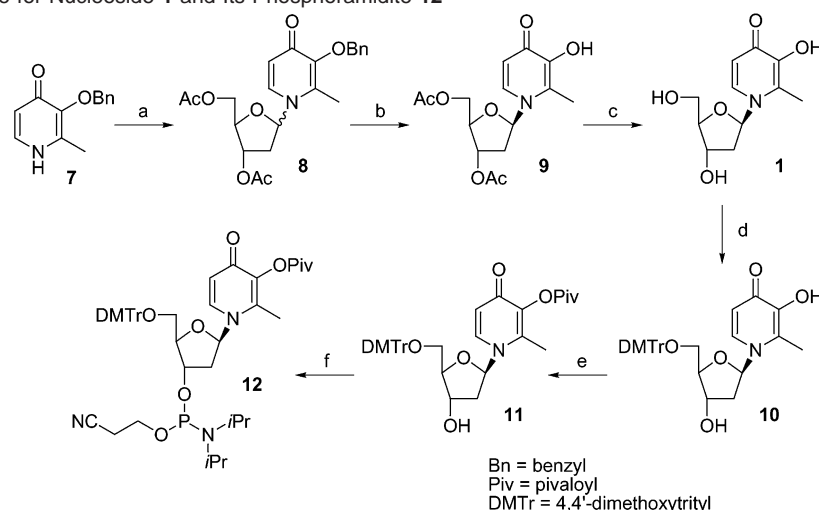
(10) Crystal data for **9**:  $\text{C}_{15}\text{H}_{19}\text{NO}_7$ , fw = 325.32, trigonal, space group  $P3_2$ ,  $a = 7.7066(3)$  Å,  $c = 44.782(1)$  Å,  $V = 2303.9(1)$  Å<sup>3</sup>,  $Z = 6$ ,  $\mu = 1.12$  cm<sup>-1</sup>,  $D_{\text{calc}} = 1.407$  g cm<sup>-3</sup>,  $F(000) = 1032.00$ . Reflection data were collected on a Rigaku RAXIS-RAPID imaging plate diffractometer with Mo K $\alpha$  radiation ( $\lambda = 0.71073$  Å) at 103 K. Of the 27 442 reflections which were collected, 5511 were unique ( $R_{\text{int}} = 0.029$ ); equivalent reflections were merged. Convergence to the final  $R$  values of  $R_1 = 0.057$ ,  $R_w = 0.095$ , and  $R_1 = 0.039$  ( $I > 2\sigma(I)$ ) for **9** was achieved by using 5502 unique reflections and 422 parameters (on  $F^2$ ), and  $R$  ( $R_w$ ) = 0.057 (0.095) for all the data. The goodness-of-fit on  $F^2$  is 1.16. The maximum and minimum peaks on the final diffraction Fourier map corresponded to 0.33 and  $-0.42$  e<sup>-</sup>/Å<sup>3</sup>, respectively.

(11) Additional  $\text{Cu}^{2+}$  ions further increased the stability only slightly.

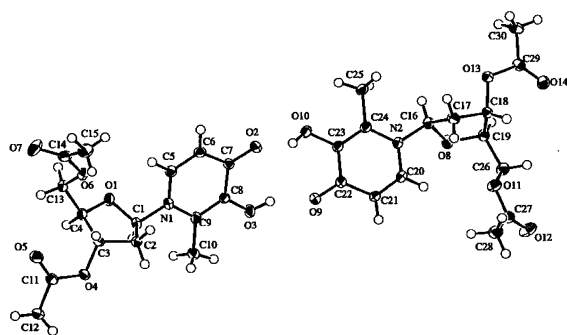
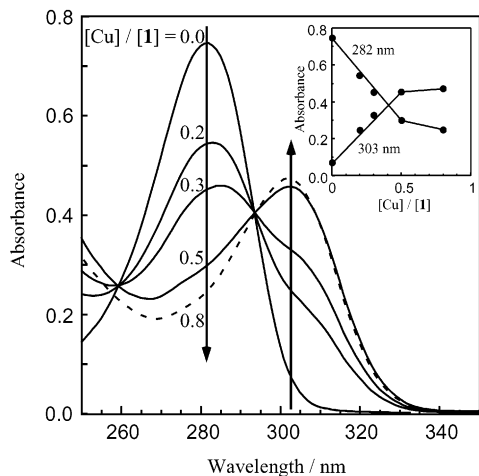
(12) It should be noted that under this condition a  $\text{Cu}^{2+}$ -mediated base pair is formed only when incorporated into DNA oligomers. For example, the binding constant determined voltammetrically for a 2:1 complex between deprotonated 1,2-dimethyl-3-hydroxy-4-pyridone ( $\text{p}K_a = 9.86 \pm 0.02$ ) and  $\text{Cu}^{2+}$  is  $\log \beta_2 = 21.7 \pm 0.8$ ; see ref 6a. The  $\text{Cu}^{2+}$  complexation inside the DNA should be reinforced cooperatively by the presence of surrounding hydrogen-bonded and stacked base pairs in the hydrophobic environment.

(13) Saenger, W. *Principles of Nucleic Acid Structure*; Springer-Verlag: New York, 1984.

(14) Wolberg, A.; Manassen, J. *J. Am. Chem. Soc.* **1970**, *92*, 2982.

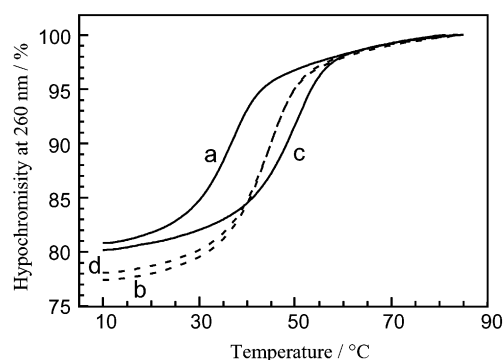
**Scheme 1.** Synthetic Route for Nucleoside **1** and Its Phosphoramidite **12**<sup>a</sup>

<sup>a</sup> Reagents and conditions: (a) (i) hexamethyldisilazane,  $(\text{NH}_4)_2\text{SO}_4$ , reflux; (ii) 1,3,5-tri-*O*-acetyl-2-deoxy-D-ribofuranose (**6**), trimethylsilyl trifluoromethanesulfonate,  $\text{CH}_3\text{CN}$ , rt, 70%; (b)  $\text{H}_2$ , Pd/C, AcOEt, rt, 30% (for  $\beta$ -anomer); (c) saturated aqueous  $\text{NH}_4\text{OH}$ , MeOH, rt, quant; (d) DMTr-Cl, pyridine, rt, 77%; (e) pivalic anhydride,  $i\text{Pr}_2\text{EtN}$ , THF, rt, 61%; (f) 2-cyanoethyl *N,N*-diisopropylchlorophosphoramidite,  $i\text{Pr}_2\text{EtN}$ ,  $\text{CH}_2\text{Cl}_2$ , rt, 61%.

**Figure 1.** ORTEP drawing for a hydrogen-bonded, paired structure of  $\beta$ -*N*-nucleoside **9** with 50% thermal ellipsoids.**Figure 2.** UV absorption changes of **1** at various concentrations of  $\text{CuSO}_4$  at 25 °C.  $[\text{I}] = 50 \mu\text{M}$  in 25 mM Na-Mops (pH 7.0). Inset: plot of absorbance at 282 and 303 nm against the ratio of  $\text{Cu}^{2+}$  to **1**.

## Conclusion

In this paper, we accomplished efficient incorporation of a neutral  $\text{Cu}^{2+}$ -mediated base pair of hydroxypyridone nucleobases into a DNA duplex. The  $\text{Cu}^{2+}$ -mediated base pair is stoichiometrically formed inside the duplex and significantly increases the thermal stability of the duplex. Nanoassembly of

**Figure 3.** Melting curves of the duplexes **2·3** (a, c) and **4·5** (b, d).  $[\mathbf{2}\cdot\mathbf{3}] = [\mathbf{4}\cdot\mathbf{5}] = 2.0 \mu\text{M}$  in 10 mM Na phosphate buffer, 50 mM NaCl (pH 7.0).  $[\text{CuSO}_4] =$  (a, b)  $0 \mu\text{M}$  and (c, d)  $2.0 \mu\text{M}$ .

multimetal arrays along the DNA helix axis is now underway toward achieving molecular wires and magnets.

## Experimental Section

**Synthesis of Hydroxypyridone-Bearing Nucleosides and Nucleotides. General Methods.** All reactions were carried out in oven-dried glasswares under nitrogen atmosphere with commercial dehydrated solvents (Wako). 1,3,5-Tri-*O*-acetyl-2-deoxy-D-ribofuranose and 2-methyl-3-(benzyloxy)-4-pyridone were prepared according to previously published procedures.<sup>8,9</sup> All other reagents were purchased and were used without further purification. Column chromatography was performed using Wakogel C-300 silica gel (Wako).

<sup>1</sup>H NMR spectra were recorded on either a JEOL EX270 (270 MHz) or a Bruker DRX500 (500 MHz) spectrometer. The spectra are referenced to TMS in chloroform-*d*<sub>3</sub>. Chemical shifts ( $\delta$ ) are reported in ppm; multiplicities are indicated by the following: s (singlet); d (doublet); dd (doublet of doublets); ddd (doublet of doublet of doublets); m (multiplet); br (broad). Coupling constants, *J*, are reported in Hz. Electrospray ionization time-of-flight (ESI-TOF) mass spectra were recorded on a Micromass LCT spectrometer.

**Compound 9.** 2-Methyl-3-(benzyloxy)-4-pyridone (**7**) (504 mg, 2.34 mmol) and a catalytic amount of  $(\text{NH}_4)_2\text{SO}_4$  were dissolved in hexamethyldisilazane (HMDS, 5 mL), and the reaction mixture was heated at reflux for 2 h before excess HMDS was distilled off. To the resulting residue was added a solution of 1,3,5-tri-*O*-acetyl-2-deoxy-D-ribofuranose (**6**) (669 mg, 2.57 mmol) in  $\text{CH}_3\text{CN}$  (25 mL). Then

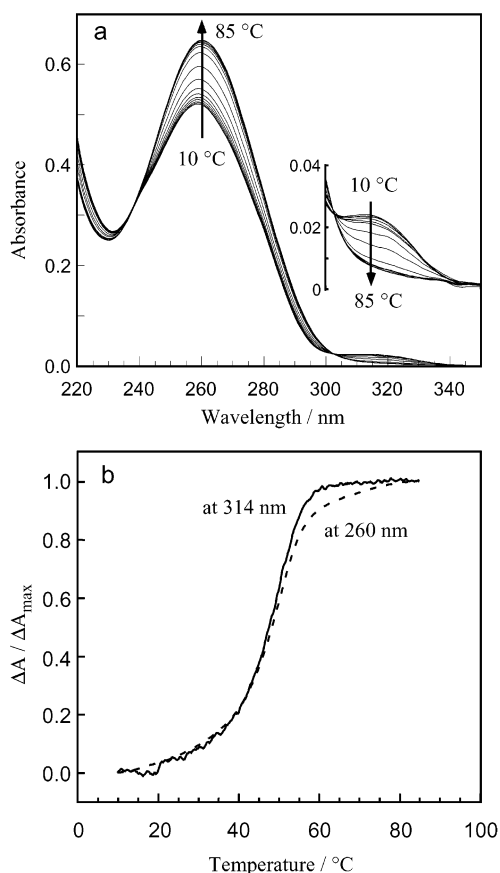


**Figure 4.** (a) Temperature dependence from 10 to 85 °C of UV absorption for the duplex **2·3** in the presence of equimolar  $\text{Cu}^{2+}$  ions.  $[\mathbf{2}\cdot\mathbf{3}] = [\text{CuSO}_4] = 2.0 \mu\text{M}$  in 10 mM Na phosphate buffer, 50 mM NaCl (pH 7.0). (b) Comparison of absorption changes ( $\Delta A/\Delta A_{\text{max}}$ ) at 260 and 314 nm (broken and solid lines, respectively).

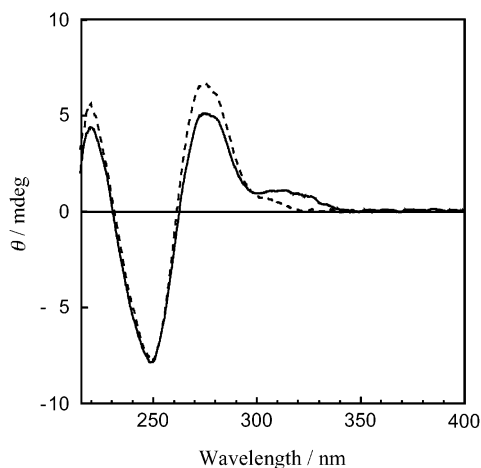


**Figure 5.** CD spectra of the duplex **2·3** in the absence (broken line) and in the presence (solid line) of equimolar  $\text{Cu}^{2+}$  ions.  $[\mathbf{2}\cdot\mathbf{3}] = 2.0 \mu\text{M}$  in 10 mM Na phosphate buffer, 50 mM NaCl (pH 7.0).

trimethylsilyl trifluoromethanesulfonate (465  $\mu\text{L}$ , 2.57 mmol) was added dropwise to the reaction mixture, and the resulting solution was stirred for 24 h at room temperature. The reaction was quenched with saturated aqueous  $\text{NaHCO}_3$  solution, and the solvent was evaporated. The residue was taken up into  $\text{CH}_2\text{Cl}_2$  and water, and the organic layer was washed with saturated aqueous  $\text{NaHCO}_3$  solution and water, dried over anhydrous  $\text{Na}_2\text{SO}_4$ , and then evaporated. Purification of the residue by silica gel column chromatography with  $\text{CHCl}_3$ – $\text{CH}_3\text{OH}$  (100:1) afforded **8** as a 3:7 mixture of  $\alpha$ - and  $\beta$ -anomers (687 mg, 70%).

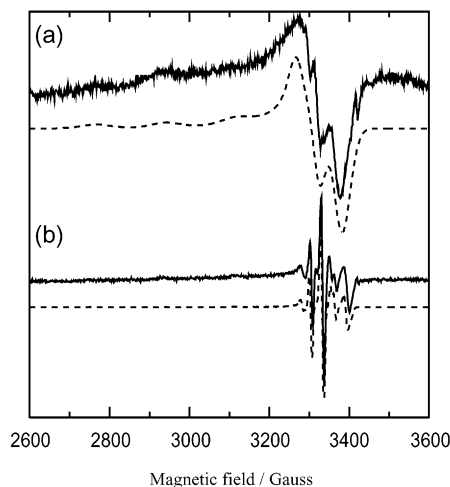


**Figure 6.** X-band EPR spectra of (a)  $\text{Cu}^{2+}$ -mononucleoside,  $\text{Cu}\cdot\mathbf{2}(\mathbf{1} - \text{H}^+)$ , and (b)  $\text{Cu}^{2+}$ -oligonucleotide,  $\text{Cu}\cdot(\mathbf{2}\cdot\mathbf{3})$ , obtained in a frozen aqueous solution at 1.5 K.  $[\text{Cu}\cdot\mathbf{2}(\mathbf{1} - \text{H}^+)] = [\text{Cu}\cdot(\mathbf{2}\cdot\mathbf{3})] = 100 \mu\text{M}$  in 10 mM HEPES, 50 mM NaCl (pH 7.0). Both spectra are reproducible by the simulation, as shown by the broken line. The parameters of the simulation are anisotropic  $g$  values:  $\text{Cu}\cdot\mathbf{2}(\mathbf{1} - \text{H}^+)$ ,  $g_x = g_y = 2.068$ ,  $g_z = 2.262$ ;  $\text{Cu}\cdot(\mathbf{2}\cdot\mathbf{3})$ ,  $g_x = g_y = 2.056$ ,  $g_z = 2.262$ , and hyperfine coupling constants of  $^{63}\text{Cu}^{\text{II}}$  nuclear spin ( $I = 3/2$ , 69.09%) and  $^{65}\text{Cu}^{\text{II}}$  ( $I = 3/2$ , 30.91%);  $\text{Cu}\cdot\mathbf{2}(\mathbf{1} - \text{H}^+)$ ,  $a_x = a_y = 1.6 \text{ mT}$ ,  $a_z = 19.3 \text{ mT}$ ;  $\text{Cu}\cdot(\mathbf{2}\cdot\mathbf{3})$ ,  $a_x = 2.8 \text{ mT}$ ,  $a_y = 2.0 \text{ mT}$ ,  $a_z = 21.4 \text{ mT}$ , where  $a_x$ ,  $a_y$ , and  $a_z$  are hyperfine coupling constants of  $^{63}\text{Cu}$  and those of  $^{65}\text{Cu}$  are multiplied by 1.07.

Compound **8** (3.7 g, 8.9 mmol) was dissolved in AcOEt (100 mL), and 10% Pd/C (500 mg, 0.47 mmol) was added to the reaction mixture. The suspended solution was stirred vigorously for 2 h under  $\text{H}_2$  atmosphere. After filtration and evaporation, the residue was recrystallized from EtOH to afford the desired  $\beta$ -*N*-nucleoside **9** as colorless plates (870 mg, 30%).  $^1\text{H NMR}$  ( $\text{CDCl}_3$ ):  $\delta$  7.68 (d,  $J = 8.1 \text{ Hz}$ , 1H), 6.45 (d,  $J = 7.6 \text{ Hz}$ , 1H), 6.01 (dd,  $J = 5.7, 7.8 \text{ Hz}$ , 1H), 5.27 (ddd,  $J = 2.4, 2.4, 6.2 \text{ Hz}$ , 1H), 4.22–4.42 (m, 3H), 2.51 (ddd,  $J = 2.7, 5.9, 14.0 \text{ Hz}$ , 1H), 2.45 (s, 3H), 2.33 (ddd,  $J = 6.8, 7.0, 7.8 \text{ Hz}$ , 1H), 2.11, 2.14 (s  $\times$  2, 6H).

**Compound 1.** To a solution of nucleoside **9** (998 mg, 3.07 mmol) in MeOH (40 mL) was added 28% aqueous  $\text{NH}_4\text{OH}$  solution (10 mL), and the mixture was stirred for 3 h at room temperature before evaporation of the solvent. The residue was solidified in AcOEt, and the colorless solid was collected (741 mg, 100%). Mp: 141.0–143.0 °C.  $^1\text{H NMR}$  ( $\text{D}_2\text{O}$ ):  $\delta$  7.95 (d,  $J = 7.5 \text{ Hz}$ , 1H), 6.50 (d,  $J = 7.5 \text{ Hz}$ , 1H), 6.21 (dd,  $J = 6.3, 6.3 \text{ Hz}$ , 1H), 4.41 (ddd,  $J = 4.4, 4.4, 6.4 \text{ Hz}$ , 1H), 4.05 (ddd,  $J = 4.4, 4.4, 8.9 \text{ Hz}$ , 1H), 3.80 (dd,  $J = 3.5, 12.6 \text{ Hz}$ , 1H), 3.71 (dd,  $J = 5.3, 12.6 \text{ Hz}$ , 1H), 2.49 (ddd,  $J = 6.6, 6.6, 13.5 \text{ Hz}$ , 1H), 2.40 (s, 3H), 2.32 (ddd,  $J = 6.5, 6.5, 13.5 \text{ Hz}$ , 1H). HRMS (FAB): calcd for  $\text{C}_{11}\text{H}_{16}\text{NO}_5$  ( $[\text{M} + \text{H}]^+$ ),  $m/z$  242.1028; found,  $m/z$  242.1023.

**Compound 10.** To a solution of nucleoside **1** (290 mg, 1.20 mmol) in anhydrous pyridine (2 mL) was added DMTr-Cl (570 mg, 1.68 mmol), and the reaction mixture was stirred for 2 h at room temperature. After the reaction was quenched with MeOH, the mixture was poured into ice–water (100 mL) and extracted with  $\text{CHCl}_3$ . The organic layer was dried over anhydrous  $\text{MgSO}_4$  and concentrated. The residue was purified by silica gel column chromatography with  $\text{CHCl}_3$ –MeOH (100:1) to obtain **10** as a colorless foam (498 mg, 77%).  $^1\text{H NMR}$  ( $\text{CDCl}_3$ ):  $\delta$  7.95 (d,  $J = 5.7 \text{ Hz}$ , 1H), 6.79–7.40 (m, 13H, including residual  $\text{CHCl}_3$ ), 6.18 (d,  $J = 7.3 \text{ Hz}$ , 1H), 6.05 (br, 1H), 4.57 (br, 1H), 4.38 (br, 1H), 4.12 (br, 1H), 3.75 (s, 6H), 2.37 (s, 3H), 2.25–2.50 (br, 2H).

**Compound 11.** To a solution of nucleoside **10** (1.05 g, 1.93 mmol) and *i*Pr<sub>2</sub>EtN (404  $\mu\text{L}$ , 2.32 mmol) in THF (7.7 mL) was added pivalic anhydride (403  $\mu\text{L}$ , 2.12 mmol), and the solution was stirred for 15 h at room temperature. The reaction mixture was poured into  $\text{CHCl}_3$  (150 mL) and washed with brine. The organic layer was dried over  $\text{MgSO}_4$

and evaporated. The residue was purified by silica gel column chromatography ( $\text{CHCl}_3$ ) and subsequent alumina column chromatography ( $\text{CHCl}_3$ ) to afford **11** as a colorless foam (741 mg, 61%).  $^1\text{H}$  NMR ( $\text{CDCl}_3$ ):  $\delta$  7.92 (d,  $J = 7.9$  Hz, 1H), 6.82–7.40 (m, 13H), 6.14 (d,  $J = 7.9$  Hz, 1H), 6.01 (dd,  $J = 6.3, 6.3$  Hz, 1H), 4.56 (br, 1H), 4.08 (br, 1H), 3.76 (s, 6H), 3.42 (br, 2H), 2.21 (s, 3H), 2.16–2.50 (br  $\times$  2, 2H), 1.37 (s, 9H).

**Compound 12.** To a solution of **11** (342 mg, 545  $\mu\text{mol}$ ) and *N,N*-diisopropylethylamine (238  $\mu\text{L}$ , 1.36 mmol) in  $\text{CHCl}_3$  (10 mL) was added dropwise 2-cyanoethyl *N,N*-diisopropylchlorophosphoramidite (267  $\mu\text{L}$ , 1.20 mmol). After 30 min, the reaction mixture was poured into ice–water (30 mL) and extracted with  $\text{CH}_2\text{Cl}_2$  (100 mL). The organic layer was washed with water, dried over  $\text{MgSO}_4$ , and then evaporated. The residue was purified by silica gel column chromatography (AcOEt containing 0.2% (v/v) pyridine) to afford a diastereomeric mixture **12** as a colorless foam (275 mg, 61%).  $^1\text{H}$  NMR ( $\text{CDCl}_3$ ):  $\delta$  7.94 (m, 2H), 6.82–7.40 (m, 13H, including residual  $\text{CHCl}_3$ ), 6.15 (m, 1H), 6.01 (m, 1H), 4.69 (br, 1H), 4.17–4.22 (br, 1H), 3.35–4.90 (m, 12H), 2.47–2.62 (m, 2H), 2.31–2.50 (br  $\times$  2, 2H), 2.27 (s, 3H), 1.40 (s, 9H), 1.08–1.21 (m, 12H).

**Oligonucleotide Synthesis.** Oligonucleotides **2–5** were synthesized on an ABI 394 DNA synthesizer using standard  $\beta$ -cyanoethyl phosphoramidite chemistry. Reagents and concentrations applied were the same as those for syntheses of natural DNA oligomers. Syntheses were performed on a 1  $\mu\text{mol}$  scale trityl-on mode, according to the manufacturer's protocol. The only change made to the usual synthesis cycle was the prolongation of the coupling time to 3 min. After the oligomers were removed from the support and deprotected by treatment with 25%  $\text{NH}_3$  (55  $^\circ\text{C}$ , 12 h), the crude oligonucleotides were purified

and detritylated by OPC protocol. The yields and concentration of solutions were determined by comparison of UV absorption at 260 nm with nearest-neighbor parameters<sup>15</sup> and molar extinction coefficient of **1** ( $\epsilon = 5.34 \times 10^3$  at 260 nm).

**UV Absorption Measurements and UV-Melting Experiments.** UV absorption spectra were recorded on a Hitachi U-3500 spectrometer equipped with a Peltier thermoelectric temperature control unit. Melting curves (at 260 nm) were recorded for a consecutive heating (10–85  $^\circ\text{C}$ ) heating–cooling–heating protocol with a linear gradient of 1.0  $^\circ\text{C}/\text{min}$ .

**Circular Dichroism Study.** Experiments were performed with a JASCO J-820 spectropolarimeter equipped with a Peltier thermoelectric temperature control unit. A 1 cm path length quartz cuvette was used for scans from 400 to 200 nm at 25  $^\circ\text{C}$ .

**EPR Study.** EPR spectra were recorded on a Bruker E500 spectrometer with an Oxford cryo-system.

**Acknowledgment.** This work is supported by Grants-in-Aid for Scientific Research (B), Nos. 13554024 and 14340206, and by that on Priority Area, No. 13128202, to M.S. from the Ministry of Education, Culture, Sports, Science, and Technology of Japan.

**Supporting Information Available:** X-ray data (in CIF format) for **9**. This material is available free of charge via the Internet at <http://pubs.acs.org>.

JA027175O

(15) Cantor, C. R.; Warshaw, M. M.; Shapiro, H. *Biopolymers* **1970**, *9*, 1059.